4

Expression of Metabolic Coupling and Adhesion Proteins in the Porcine Optic-Nerve Head: Relevance to a Flow Model of Glaucoma

Francisco-Javier Carreras[1], David Porcel[2], Francisco Rodriguez-Hurtado[3], Antonio Zarzuelo[4], Ignacio Carreras[1] and Milagros Galisteo[4]
[1]*Department of Surgery (Ophthalmology), Faculty of Medicine, University of Granada*
[2]*Center of Scientific Instrumentation, University of Granada,*
[3]*Division of Ophthalmology, Licinio de la Fuente University Hospital, Granada,*
[4]*Department of Pharmacology, Faculty of Pharmacy, University of Granada,*
Spain

1. Introduction

Astrocytes perform several well-established homeostatic functions in the maintenance of a nervous system that is viable for neurons. These functions include: the provision of metabolic support for neurons; maintenance of the blood-brain barrier (BBB); absorption of K+ and neurotransmitters from extracellular spaces; and participation in the processes of synaptogenesis and angiogenesis (Wanga & Bordey, 2008)

Astrocytic processes send out projections towards blood vessels that terminate in prolongations called endfeet. These express on the membrane a specific form of glucose transporter, GLUT1 (Morgello et al., 1995; Yu & Ding, 1998). Astrocytes take glucose from blood and transfer it to neurons, but it is also now known that an O_2 limitation is not a requirement for the formation of l-lactate in the cell metabolism. It is becoming increasingly clear that neurons utilize different substrates (glucose, glycogen, and lactate) to support their metabolism (Brown et al., 2004; Brooks, 2009), although this process may depend on the surrounding conditions. Lactate is an important intermediary in aerobic glucose metabolism, and a mediator of the redox state in intracellular and extracellular compartments (Brown et al., 2004). Specifically, l-lactate and molecular transporters (monocarboxylate translocator isoforms or MCT) play an important role in the metabolism of mitochondria (Pasarella et al. 2008). It has been proposed that l-lactate is the main product of glycolysis in the brain, regardless of the presence of oxygen (Brooks, 2002; Schurr, 2006)).

It has been shown that all isoenzymes of LDH, LDH1-LDH5 are present in varying proportions in synaptic terminals and cultured neurons and astrocytes taken from the brain. In rats, there is a selective enrichment of LDH1 in synaptosomes and LDH5 in astrocytes, although there is no exclusive localization of isoenzymes. The production of lactate by astrocytes and its subsequent use by nerve endings for energy production and neurotransmitter synthesis has been suggested (O'Brien et al., 2007).

A model known as the astrocyte-neuron lactate shuttle hypothesis (Pellerin & Magistretti, 1994) proposes that glucose taken up by astrocytic GLUT1 is partly processed oxidatively

(via the tricarboxylic acid cycle pathway), partly converted to lactate, and then carried to extracellular spaces via monocarboxylate transporters (MCT1). Once in an extracellular space, l-lactate is then transported into neurons via MCT2 and converted to pyruvate (which can be used in the tricarboxylic acid cycle (Pellerini et al., 2007a)). The production and release of lactate by Müller cells in the retina has been found to fuel the mitochondrial oxidative metabolism and glutamate resynthesis in photoreceptors. Lactate has been found to be a better substrate than glucose for the oxidative metabolism *in vitro* for the Müller cell-photoreceptor complex (Poitry-Yamate et al., 1995). Recent *in vivo* studies in humans suggest that lactate may be preferred to glucose as fuel for neuronal metabolism (Brooks, 2009; Smith et al., 2003). Alternative approaches for improving energy metabolism in neurons based on astrocyte-neuron interactions, such as enhancing lactate uptake in neurons, or confronting challenges to these vias, may constitute the basis for new therapeutic strategies for neuroprotection (Smith et al.,2003).

Except for vessels and microglia, the anterior surface of the optic nerve head is formed by only one type of astrocyte with slight though significant differences that depend on the zone of settlement in relation to axons. The main difference between two subgroups of stellate astrocytes that form the anterior part of the optic nerve head may be their relative commitment either to envelope axons or merely to become part of the contingent surrounding vessels where axons are absent. Membrane adhesion is a critical feature of the astrocyte-astrocyte and axon-astrocyte relationship. Membrane-adhesion molecules are key to the axon-astrocyte proximity that enable metabolic enzymes and transport molecules to function in the nutrition chain of the neuron. N-cadherin has been described as a major linking protein for the two subgroups of stellate astrocytes in the prelaminar tissue of the optic nerve during development (Redies & Takeichi, 1993). N-cadherin participates both in complex and in simple attachments between membranes in the adult optic nerve head (Carreras et al., 2009, 2010a).

In the study of the pathology of the circulation of aqueous humor, clinically manifested in distinct types of glaucoma, considerable emphasis has been placed on changes in intraocular pressure. As a consequence of less outflow ease through conventional pathways, a redirection of flow towards alternative pathways reportedly occurs. The resulting pharmacological possibilities have been exploited by a group of drugs that reduce intraocular pressure by increasing uveoscleral outflow(Alma & Nilsson, 2009). However, deviation of flow towards the posterior pole has not been thoroughly investigated. Recently, a pathogenic role for a postulated greater outflow through the optic nerve head has been proposed, and N-cadherin has been suggested as a possible target for ionic stress in the optic nerve head (Carreras et al., 2009). In support of this, permeability of the optic-nerve head to tracers has also been recently corroborated (Carreras et al., 2010b).

Neurons have different types of self-destruct programs that are spatially compartmentalized, and one of these programs is located in the axon. Compartmentalized autonomous axonal self-destruction has been proposed as an optic-nerve occurrence in glaucoma (Whitmore et al., 2005). Local noxae constricted to the prelaminar tissue would suffice to interrupt the continuity of axons. Here we explore possible mechanisms through which a reduced extracellular concentration of calcium in the prelaminar tissue caused by the occasional (pathological) flow of aqueous humor through the optic nerve head could interfere with axon metabolism. The maintenance of narrow spaces between the membranes of the astrocytes and axons is essential for the interchange of metabolic fuel mediated by transport molecules. Research on the kinetics of lactate uptake in the brain (Aubert et al., 2005) has shown that this transport depends on the lactate concentration itself in the extracellular space.

We reasoned that the reinforced presence of N-cadherin may be linked to the presence of the monocarboxylic acid transport chain in the same area. If so, in areas where axons are not present, such as the perivascular region, which is composed only of astrocytes, we would expect to find no evidence of a monocarboxylic acid transport chain, and the concentration of N-cadherin would also be lower. If evidence for the lactate-transport chain in the axonal region of the prelaminar optic nerve head is concurrent with the presence of increased amounts of N-cadherin, compared to that of the perivascular areas, this could reinforce the suggestion that the deviation of bulk aqueous flow through the optic nerve could be harmful. The aqueous humor, low in calcium, would interfere with cell-cell adhesion and the transmembrane metabolic shuttle.

In this paper, we study the presence of enzymes involved in the lactate shuttle in the optic nerve head, seeking to colocalize the main molecule responsible for the maintenance of tight extracellular spaces. The study focuses on N-cadherin distribution in the prelaminar optic nerve head tissue, with the aim of colocalizing the MCT1 and MCT2 transport molecules, as well as LDH 1 and LDH 5, the main enzymes responsible for lactate metabolism in astrocytes and neurons. MCT1 and MCT2 are transmembrane proteins expressed in small amounts on the cell surface. Compared to prevalent proteins in axons and astrocytes as neurofilament and glial fibrillary acidic protein fluorescence of MCTs is expected to be very reduced, and prior identification by Western blot is helpful. Once its presence is determined in the tissue, histological localization with immunofluorescence allows comparisons of the tissue distribution of both N-cadherin and MCTs.

We found MCT1 and 2 in astrocytes and neurons, but membrane localization with TEM immunolabeling, although suggestive, by itself is not informative of the precise distribution of the two isoforms among the two cellular types, astrocytes, and neurons. Organotypic culture of the excised prelaminar region of the optic-nerve head can be useful in ascertaining the distribution of MCTs: first, the survival of astrocytes in organotypic culture is established; simultaneously the timing of axonal destruction is monitored; and, finally, MCTs are quantitatively determined by Western blot in control tissue and after axon disintegration. Comparisons of the amount of MCTs both in the presence an absence of axons elucidates the distribution of those transport molecules between the astrocytes and neurons (axons).

2. Methods

2.1 Animals

For this study, a total of 83 eyes from six-month-old domestic pig were collected at an abattoir soon after the animals were killed. The time between the death of the animals and processing of the tissue averaged less than 3 h. Eyes for the morphological study were processed in the first hour after death. The procedures followed in this research adhered to the tenets of the Helsinki Declaration.

Five eyes were used to determine the presence of MCT1 and MCT2 in normal tissue by Western blot.

Fresh eyes were dissected with blades and scissors. The optic nerve was prepared for transmission electron microscopy (TEM) and confocal laser scanning microscopy (CLSM). Immunostaining was performed for CLSM and TEM. For TEM, 8 eyes were prepared: 4 for immunogold staining, and another 4 for conventional TEM. Five eyes were used for CLSM. Thirty-six eyes were used for the organotypic culture of the prelaminar optic nerve head and processed for morphological assessment by immunolabeling and CLSM.

Finally, 28 pig eyes were used for the organotypic culture of the prelaminar optic nerve head and processed for Western blot of MCT 1, MCT 2 and a control protein (β-actin). Additionally, 4 eyes from 4 normal Wistar rats (from a different experiment), were used as positive controls for the detection of MCT1 and MCT in the optic disc in order to test the efficacy of the antibodies. Results were positive (not shown).

2.2 Antibodies and staining reagents

The following specific primary antibodies were used: anti-neurofilament, anti- GFAP (Glial Fibrillary Acidic Protein), anti-N-cadherin, anti-LDH5, anti-LDH1, anti-MCT1, and anti-MCT2. Secondary antibodies were labeled with fluorescent dyes (FITC or Texas red) for CLSM, or with colloidal gold for TEM. Secondary antibody for Western blot was labeled with horseradish peroxidase and revealed with luminol as substrate (ECL Western Blotting Substrate kit from abcam lab). Information on the antibodies used is presented in Table 1. Several assays were performed until operative working solutions were obtained. The most used dilutions are listed in table 1. Nuclear counterstaining for CLSM was performed with mounting media using DAPI (Vectashield, Vector Laboratories, CA, USA).

2.3 Confocal laser scanning microscopy (CLSM)

General procedure: The tissues were immunostained by fixing in glyoxal (Shandon Lipshaw, Pittsburgh, PA, USA) and then processed for paraffin embedding. Sections 5 μm thick were cut and mounted on polylysine-coated plates. Serial sections were washed in PBS after deparaffinization with xylene and graded alcohol. The sections were incubated in pre-diluted block serum for 1 h, and then incubated with the primary antibody diluted overnight in PBS containing 1.5% blocking serum, at4ºC. Control sections that did not receive the primary antibody were maintained with block serum. Primary antibodies were monoclonal antibodies against neurofilament, N-cadherin, LDH5, LDH1, MCT1, and MCT2. The secondary antibody was chosen as shown in Table 1, and incubation was performed for 1 h at room temperature. After being mounted with Vectashield, the sections were observed and photographed using a Leica SP5 confocal laser microscope.

2.4 Statistical analysis of immunofluorescent density

The first step was to study the distribution of the axons in the prelaminar optic nerve head with anti-neurofilament. Ten sections from 5 eyes (from different animals) were then incubated with anti-N-cadherin antibody as detailed above. The secondary antibody was marked with FITC. Two additional sections received only the secondary antibody and were used as controls. The sections were examined and photographed in such a way that at least one major vessel was present in each photograph. Low magnification (200 x) was used to include the vessel and the fiber layer in the same picture. Digital images were collected by adjusting the sensitivity of the photomultiplier according to the fluorescent intensity of the negative control section incubated with the secondary antibody, but not with the primary antibody. Once established, the same parameters were used to explore the sections incubated with the primary and secondary antibodies. Selection of the areas was based on the morphology of the tissue and the distribution of the DAPI-stained nuclei . Using the results of the anti-neurofilament labeling as reference, we distinguished areas with axons and astrocytes (axonal areas) as well as areas with only astrocytes (perivascular). Fluorescent intensity was measured in three or (mainly) four locations in each region of each picture (depending on the area available).

Antibody	Laboratory	Species	Label	Final dilution	Proven reactivity
Anti-GFAP	Abcam	Mouse IgG	Alexa Fluor 594	Prediluted	human, rat, pig
Anti-GFAP	eBioscience	Mouse IgG	Alexa Fluor 488	2.5 μg/ml	chicken, monkey, rabbit, human, mouse, rat, pig
Anti-N Cadherin Secondary antib.	Sigma-Aldrich Sigma-Aldrich	Mouse IgG Goat anti-mouse	FITC	1/100 1/200	chicken, monkey, rabbit, human, mouse, rat
Anti-Neurofilament Secondary antib.	Sigma-Aldrich Sigma-Aldrich	Mouse IgG Goat anti-mouse	FITC	1/50 1/100	wide range
Anti-Neurofilament	Santa Cruz Tech	Goat anti-human		1/50	human, mouse, rat
Secondary antib.	Santa Cruz Tech	Mouse-antigoat		1/100	
Anti-LDH 1 Secondary antib.	Sigma-Aldrich Sigma-Aldrich Abcam	Mouse IgG Anti-mouse IgG Anti-mouse IgG	FITC Texas Red	1/100 1/200 1/500	human
Anti-LDH 5 Secondary antib.	Abcam Abcam	Sheep IgG Rabbit anti-sheep	Texas Red	1/100 1/500	
Anti-MCT 1 Secondary antib.	Santa Cruz Tech Santa Cruz Tech Sigma-Aldrich	Goat IgG Donkey anti-goat Rabbit anti-goat	FITC Gold	1/100 1/100 1/75	mouse, rat, cow, human
Anti-MCT 2 Secondary a.	Santa Cruz Tech Santa Cruz Tech Santa Cruz Tech	Rabbit IgG Goat anti-rabbit Goat anti-rabbit	Texas Red Gold 10 nm	1/100 1/100 1/75	mouse, rat

Table 1. List of antibodies for Immunostaining

Image Pro Plus 6.3 (Media Cybernetics, MD, USA) was used to analyze the photographs. The "line profile" command was used to plot the intensity values of a single circular line within the image (along a single line of pixels). It is important to note that the line profile measures pixel values as they appear in the bitmapped image. After selecting only the green channel, the program plots only the values for FITC fluorescence. Because part of the spectrum of DAPI can overlap the green channel, care was taken to avoid placing the line (circumference) on top of the blue-stained nuclei. Pooled data from each area in each section was recorded as ± SE, and statistical differences were assessed using the Student's t-test.

2.5 Transmission electron microscopy

The prelaminar region of the optic nerve head and the adjacent retina were sectioned with a Parker blade and deposited in fixative. For a simple TEM, 2% glutaraldehyde and 2% formaldehyde in a PBS buffer were used as a fixative. After fixation, the specimens were rinsed several times with a buffer solution followed by post-fixation with 1% osmium tetroxide for 1 h. After rinsing again with PBS buffer for 15 min, the tissue specimens were dehydrated with a series of graded ethyl alcohols ranging from 70% to 100%. The blocks were embedded in epoxy resin. The resin blocks were initially thick-sectioned at 1-2 microns with glass knives, using an Ultramicrotome Leica Ultracut S, and stained with Toluidine blue. These sections were used as a reference to trim blocks for thin sectioning. The appropriate blocks were then thin sectioned with a diamond knife at 70-90 nm, and the sections were placed on nickel mesh grids. After drying on filter paper, the sections were stained with uranyl acetate and lead citrate for contrast. After drying, the grids were then viewed and photographed using a Zeiss EM 10C electronic microscope.

For immune procedures, tissue was fixed with 2% paraformaldehyde and 0.2% glutaraldehyde in PBS. For better preservation of antigenicity, no osmium tetroxide was used. London White embedding resin was used. The grids were incubated with the secondary antibody as a control, but they were not incubated with the primary antibody. The grids were incubated in block serum for 10 min. The sections were then incubated overnight with the primary antibody (anti-MCT1 and anti-MCT 2; see Table 1). The same primary monoclonals were used for TEM and confocal laser microscopy. The washed grids were then incubated with the secondary antibody labeled with nanogold 10 nm. After drying on filter paper, the sections were stained with uranyl acetate for contrast. No lead citrate was used so as to avoid masking the gold marker.

2.6 Organotypic culture of prelaminar optic-nerve explants

Explants of the dissected prelaminar region of the optic nerve head of recently enucleated pig eyes were cultured *in vitro* following the method described by Stoppini et al. (1991) as adapted by Carrasco et al. (2010).

Briefly, optic discs were dissected with a surgical blade in a sterile environment and placed in a Petri dish containing the same culture medium as detailed below. Explants were subsequently placed on 30-mm Millicell CM culture plate inserts (Millipore, Billerica, MA, USA; pore size 0.4 μm) in 6-well plates containing 1 ml/well culture medium and incubated *in vitro* for different time periods (see below) at 37ºC in a humidified atmosphere with 5% CO2. The face of the explant in contact with the membrane was not controlled. The medium was replaced after 24 or 48 h, coinciding with the harvesting of the samples. The culture medium was composed of 50% basal medium with Earle's salts (BME), 25% Hank's balanced salt

solution, 10% horse serum (HS), 1 mM L-glutamine, 10 IU-µg/ml penicillin-streptomycin (all purchased from Invitrogen, Paisley, United Kingdom), and 5 mg/ml glucose (BME+25%HS).
A total of 64 eyes were used in this phase of the study. Optic-nerve explants were incubated in groups of variable number of samples.
For morphological studies of viability of axons and astrocytes a total of 36 eyes were studied, including 6 control eyes (0 days of culture). Initially, explants were retired daily for the first 4 days an then every 2 days up to day 12. After experience concerning the rate of desintegration of the axons in the culture was gained, we cultured 6 explants for 24 h and then prepared for histological study. Samples were fixed in Glyoxal for 24 and then either immersed in 30% glucose and included in OCT and frozen. Another similar culture was alternatively processed for paraffin embedding. In both cases, sections of the embedded tissue were labeled with fluorescent antibodies against Neurofilament or GFAP and observed in the CLSM. Counterstaining was consistently DAPI, as stated above.

Antibody	Laboratory	Species	Label	Final dilution	Proven reactivity
Anti-MCT 1	Abcam	mouse		1/400	mouse, rat, cow, human
Anti-MCT 2	Abcam	mouse		1/400	mouse, rat, cow, human
Secondary antib.	Sigma	goat	HRP	1/1000	

Table 2. List of antibodies for Western blot.

2.7 Western-blot analysis for MCT1 and MCT2 expression in prelaminar optic nerve

For protein immunoblot determination, an initial Western-blot analysis was performed in 5 fresh samples to determine the presence or absence of MCT1 and MCT2 in the prelaminar optic nerve of the pig.
To determine the distribution of MCT isoforms, we processed an additional group of 28 eyes, including 6 controls (not cultured) and 22 cultured eyes. Samples were harvested at days 1 (24 h), 2, and 5 . From prior immunolabeling histological results, we knew that axons disintegrated after one day of culture. A quantitative comparison between cultured and control samples was calculated to determine the proportional distribution of MCT1 and MCT2 between axons and neurons. Western-blot analysis was performed in control tissue from untreated normal pigs. The analysis was repeated after organotypic culture of the prelaminar optic nerve for a number of days (1, 2 and 5) until the disintegration of the axons was tested with immunolabeling of neurofilament, as discussed above.
Samples of the prelaminar region of the optic nerve head, control or cultured, were homogenized in buffer (20 mmol/L Tris-HCl, 5mmol/L EDTA, pH 7.5, 10mmol/L sodium pyrophosphate, 100 mmol/L sodium fluoride, 1% (v/v) Igepal, 2 mmol/L sodium orthovanadate, 1 mmol/L phenylmethylsulfonyl fluoride, 10 µg/ml aprotinin and 10 µg/ml leupeptin). Homogenates were centrifuged at 14,000 rpm for 10 min at 4ºC. Protein concentrations in homogenates were measured by the bicinchoninic acid protein assay. Thirty µg of protein of each sample were subjected to 10% SDS-PAGE and electrophoretically transferred to nitrocellulose membranes overnight. The membranes were blocked with 5% non-fat dry milk in TBST for 2 h at room temperature and subsequently

blotted with the appropriate antibodies in 5% non-fat dry milk-TBST. The antibodies anti-MCT1, and anti-MCT2, were purchased from Abcam (Cambridge, UK) and were used at manufacturer-recommended dilutions (1/400). Incubations with primary antibodies were performed overnight at4ºC. Following incubation, membranes were washed 3 times with TBST for 10 min each, before incubation for 2 h at room temperature with secondary peroxidase conjugated anti-mouse antibody, in the case of MCT1 (Santa Cruz Biotechnology, Santa Cruz, CA, USA), or anti-rabbit antibody, in the case of MCT2 (Santa Cruz Biotechnology, Santa Cruz, CA, USA) diluted at 1:2000 in 5% non-fat dry milk-TBST. Membranes were then washed 5 times with TBST for 10 min each, and the bound antibodies were visualized by an ECL system. Films were scanned and densitometric analysis was performed on the scanned images using Scion Image-Release Beta 4.02 software (*http://www.scioncorp.com*). Antibodies used are summarized in table 2.
Aquantitative comparison between cultured an control sample was calculated in the following manner: relative values were expressed as means, indicating the values from densitometric analysis normalized to Ponceau red staining, relative to control measurements, which were assigned a value of 100.

3. Results

3.1 Protein immunoblot of complete tissue

The Western-blot results from normal fresh tissue for MCt1 and MCT2 rendered specific positive results for both molecules. A stained band in the region below the mark of 50 KDa indicated the presence of types 1 and 2 of the monocarboxylate transporter (Fig. 1).

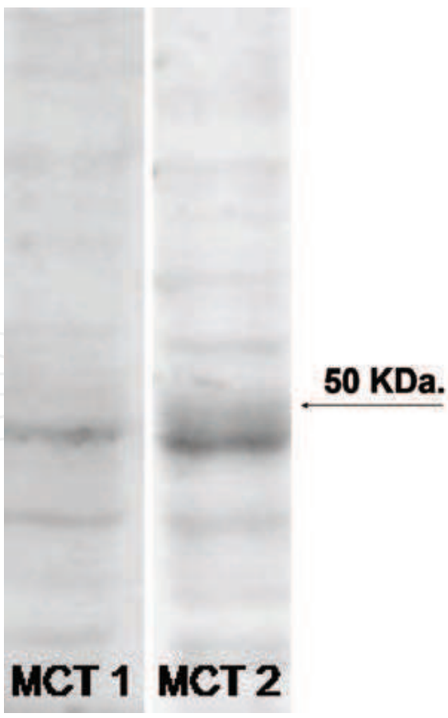

Fig. 1. Western blot detection of MCT-1 and MCT2 in the bands well under 50 k Daltons from fresh tissue samples of the prelaminar region of the porcine optic-nerve head.

3.2 Normal histology

Qualitative assessment. Fluorescence intensity was scored on a **qualitative** scale: - negative; +/- borderline; + weakly positive; + + positive; +++ strongly positive.

3.2.1 Immunolabeling of the neurofilament and GFAP

Qualitative assessment of neurofilament staining was strongly positive. Immunolabeling for the neurofilament clearly separated areas with and without axons in the optic nerve head sections (Figure 2a). Apart from the vessel walls, perivascular tissue was formed almost exclusively of astrocytes and no axons were present. The perivascular tissue was composed of Elschnig's astrocytes, which also formed the superficial Elschnig's "membrane" and the astrocytes of the meniscus of Kuhnt in the center of the optic disc. Figure 2a shows the course of axons in the optic nerve head and the nuclei of the astrocytes. Some of the astrocytes tended to gather in columns on each side of the axon bundles. Another group of astrocytes was situated around the main vessels. No immunofluorescence was found in the spaces near the vessels. Two arrangements of astrocytes – from the standpoint of their relationship to axons – could be distinguished using neurofilament immunofluorescence: perivascular astrocytes and axon-related astrocytes.

Qualitative assessment of GFAP staining was strongly positive (Figure 2b). Of particular interest in our work was the determination of whether the segment of the fiber bundles piercing the *lamina cribr*osa was still the domain of axon-wrapping astrocytes, because the most intense staining of MCT molecules was rendered in this area. Our results show that astrocytes, and consequently not oligodendrocytes, were present in the tunnels of the *lamina cribrosa* (Fig 2b, long arrow).

3.2.2 TEM of zonulae adherens

A conventional TEM of the prelaminar tissue of the optic nerve head shows important structural differences in the perivascular and axonal layers. Perivascular astrocytes, unrelated to axons, formed a mesh of astrocytic projections, with ample extracellular spaces (Figure 3). Periaxonal astrocytes sent out projections that tightly wrapped around nerve fibers, leaving barely discernible extracellular spaces (Figure 4). Figures of zonulae adherens were found among the astrocytic projections in both areas, but not in the same numbers. The vast majority of the membrane contacts among projections in the perivascular area were simple membrane apposition (Figure 3b). Union complexes of the zonula adherens type were structured unions with extracellular and intracellular elements that produced a characteristic five-layered image in TEM. Zonulae adherens were occasionally found among perivascular astrocytes (Figure 3c), but were more numerous among periaxonal astrocytes where cellular contact was close. Zonulae adherens were seen to predominate near the axons joining thin astrocytic processes in several layers around the neural fibers (Figures 4b and c).

3.2.3 Immunolabeling of N-cadherin

Qualitative assessment of N-cadherin staining was strongly positive. Since the main extracellular component of zonula adherens is N-cadherin, the immunolabeling of N-cadherin is a suitable method for studying the distribution of zonulae adherens at the CLSM level. After the immunostaining of sections of the optic nerve head, N-cadherin staining was positive in areas of the prelaminar region, but intense fluorescence occurred in the

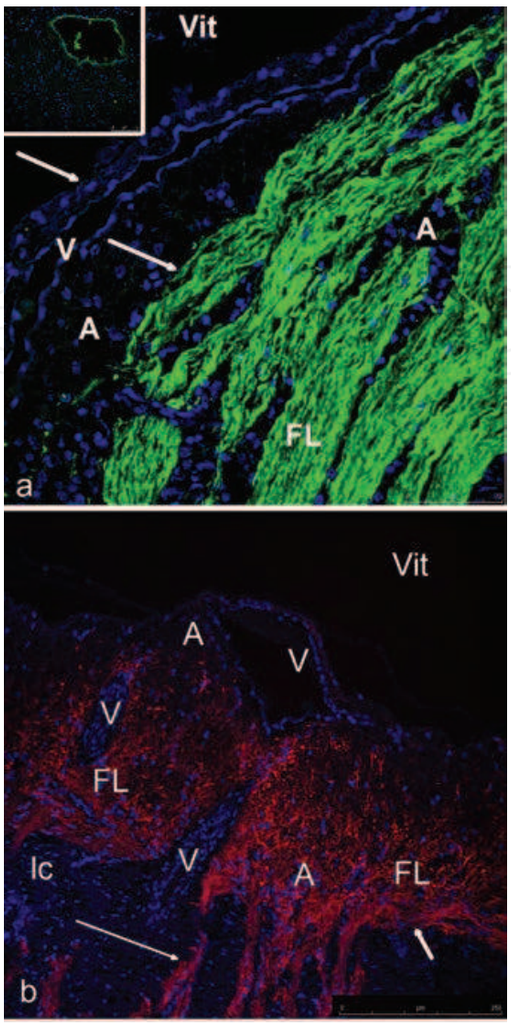

Fig. 2. a) Confocal laser scanning micrograph of a section of the anterior part of the optic nerve head in contact with the vitreous body stained with fluorescent antibodies directed against an anti-neurofilament antibody. The result is a clear indication of the flow of axons in the optic nerve head. Axons are shown to form clearly delimited bundles interspersed with columnar astrocytes. The astrocytes are only detected above by the blue counterstaining of their nuclei (DAPI). A vessel is present in the upper third if the micrograph shows that no green dye is present, thereby indicating the absence of axons in this area. Astrocytic nuclei are numerous in the proximity of the vessel. These are the astrocytes described by Elschnig as responsible for the formation of the incomplete inner limiting membrane of the optic nerve. White arrows indicate the limits between the vitreous surface and the fiber layer. b) Confocal laser scanning micrograph of a section optic nerve head, including the lamina cribrosa, stained with fluorescent antibodies directed against an anti-GFAP antibody. Astrocytes strongly express GFAP. The short arrow points to the upper limit of the sclera where the horizontal portion of the fiber layer lies. The long arrows point towards the bundles piercing the holes of the lamina where intense GFAP staining shows that the axons at the lamina are still wrapped by astrocytes instead of oligodendrites. (**Vit**: Vitreous body; **V**: Vessel; **A**: Astrocytes; **FL**: Fiber layer).

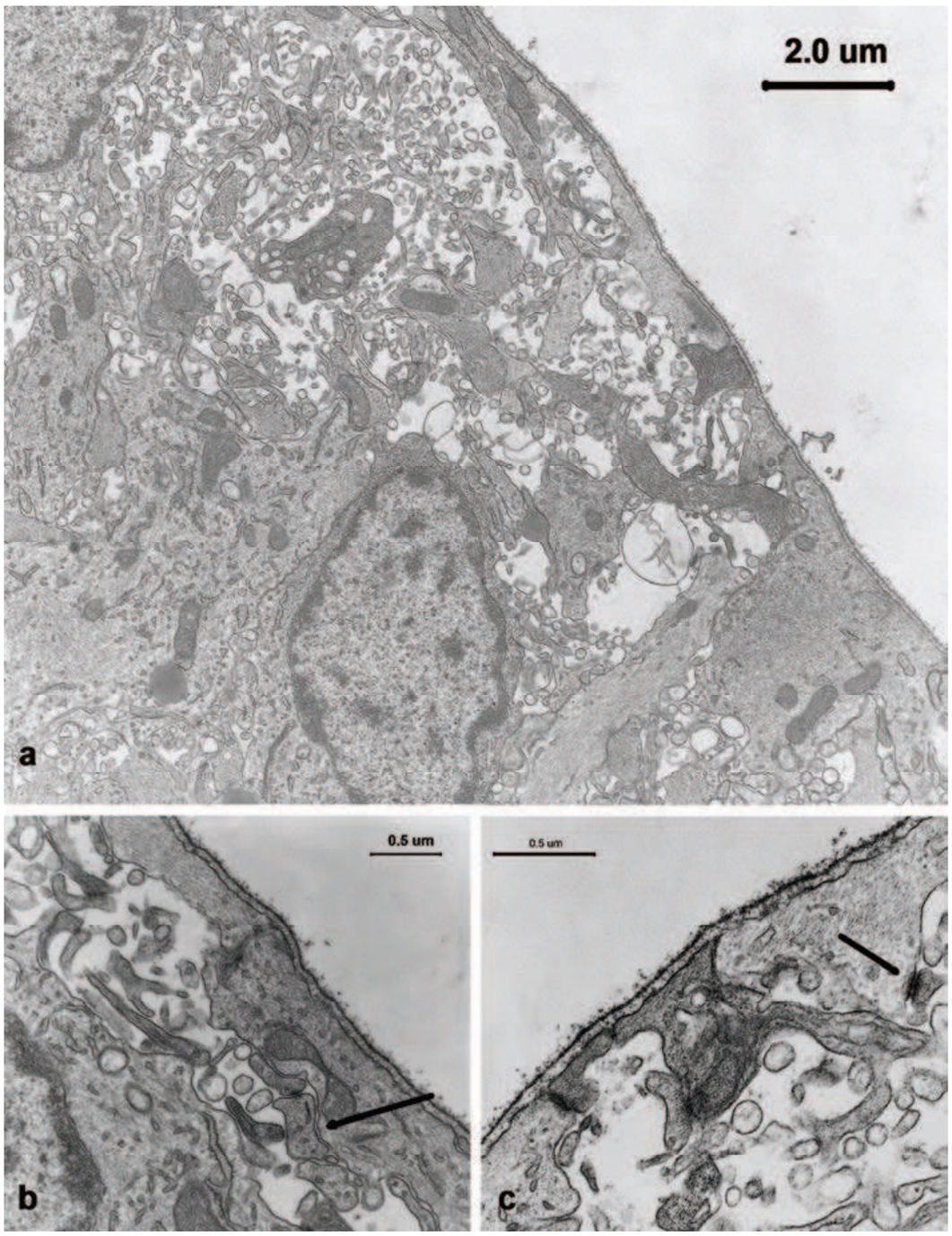

Fig. 3. TEM micrograph of Elschnig's perivascular astrocytes . a) Astrocytes forming the vitreous interface. Ample extracellular spaces are present among the astrocytic prolongations; and it is from these spaces that free-floating lesser projections arise. No axons are present in the area near the vessel wall. b) A close view of the membrane-to-membrane contact. The most common form of attachment between membranes is simple membrane apposition (arrow). c) This micrograph shows that structured forms of attachment, such as zonulae adherens, are occasionally found in this area (arrow). (**Vit**: Vitreous body; **A**: Astrocytes).

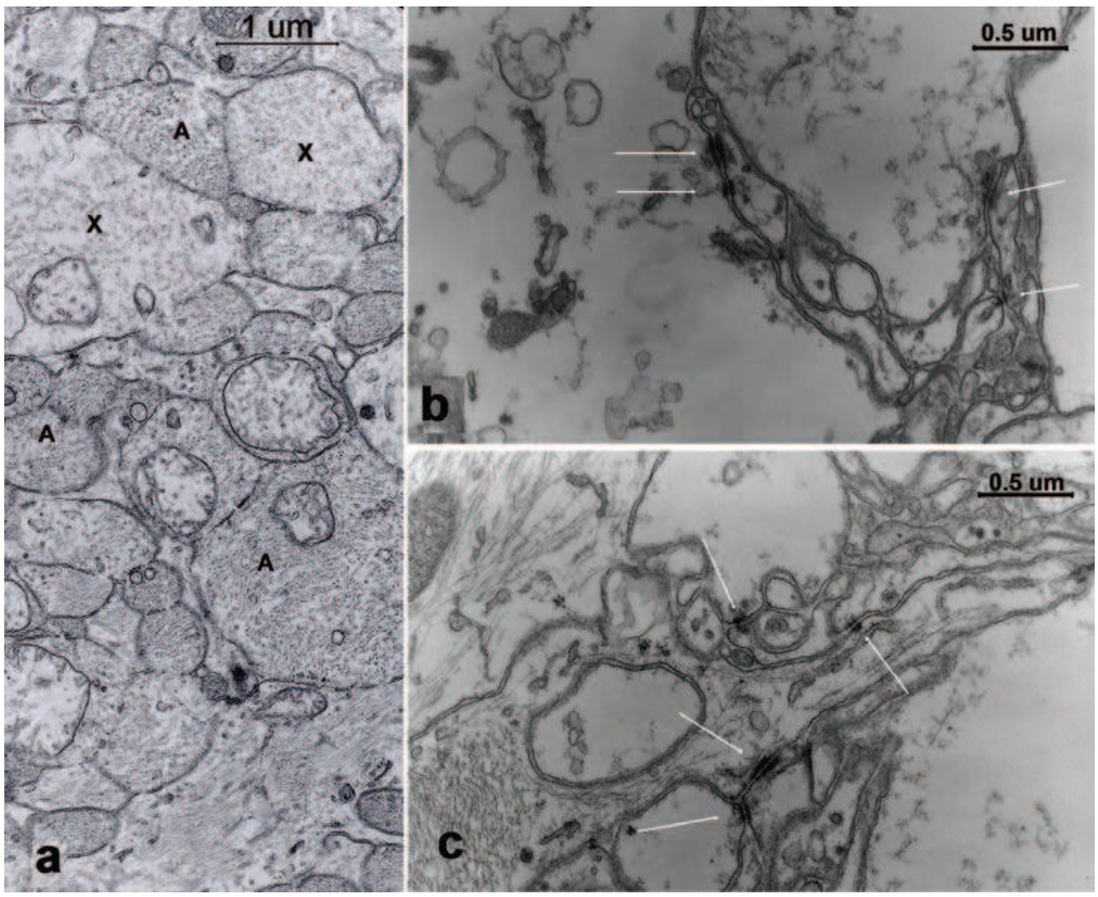

Fig. 4. TEM micrograph of the periaxonal astrocytes in the nerve-fiber layer. a) A general view of the axon-astrocyte relationship. All the spaces unoccupied by axons (X) are filled with thin astrocytic processes (A). Extracellular spaces are slit-like and scarce. b) and c) A close-up view of the membrane-to-membrane contact between axons and astrocytes. Astrocytic prolongations form multi-layered structures surrounding axons. Zonulae adherens are frequently found. (Compare with Figure 2, in which only isolated and scarce figures of zonulae adherens are found.) Figures of zonulae adherens are grouped together, and the thin-layered astrocytic prolongations are tightly wrapped around axons (arrows). These details should be taken into account when interpreting the non-contrasted immunogold micrographs shown in Figures 9 and 10.

nerve-fiber layer. The distribution of N-cadherin suggests a moderate presence of zonulae adherens among perivascular astrocytes (Elschnig's cover and Kuhnt's meniscus), pointing to an increased concentration in the ganglion cell-fiber columns (Figure 5). These results concur with previous findings with TEM.

Due to the uncertainties inherent in TEM immunolabeling, a quantitative approach using this technique is fraught with difficulties. However, quantitative immunofluorescence has been greatly facilitated by the development of image-analysis software. Accordingly, a quantitative approach to the relative concentration of N-cadherin labeling was used as a method to discern the relative concentration of zonulae adherens among astrocytes in the perivascular area and those in the fiber layer.

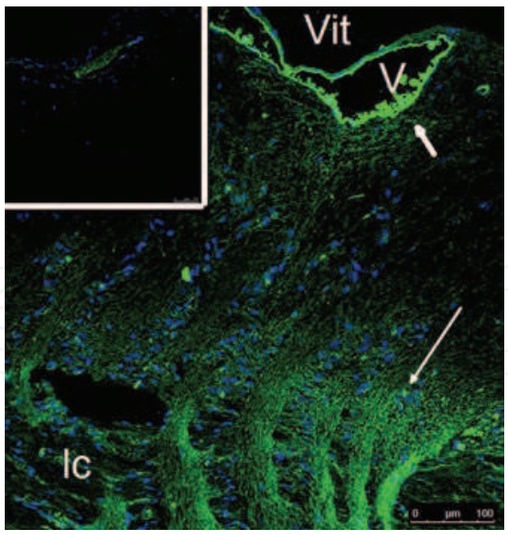

Fig. 5. CLSM of distribution of N-cadherin in the prelaminar region. N-cadherin is present in Elschnig's perivascular astrocytes (short arrows) and in periaxonal astrocytes (long arrows). Background noise has been eliminated. Magnification is shown in the figure. (**V**: vessel; **ca**: columnar astrocytes; **lc**: lamina cribrosa; and **sc**: sclera).

3.2.4 Statistical comparison of the intensity of N-cadherin immunofluorescence between perivascular astrocytes and axon-wrapping astrocytes

A statistical analysis examined data on fluorescent intensity along lines drawn in the two areas under comparison: namely, the perivascular area and the nerve-fiber layer. Figure 6 shows an example of the preparations used in the statistical analysis. The squares show the areas where the labeling intensity was measured. Figure 6a shows the intensity profiles for the selected lines of two identical squares, at a random location situated in each of the anatomically defined areas under comparison, and shown in Figure 6b. This figure is a sample photograph of one of the sections which was immunolabeled for N-cadherin.

Circular lines instead of straight lines were used for statistical calculations (this is a constraint of the software). Circular lines of the same length and traced with the "line profile" command in the software package were randomly placed in both regions and the average intensities compared. The results of the statistical labeling analysis are shown in Table 3. Statistical analysis of the measurements of fluorescent intensity along the lines

Parameter:	PERIVASCULAR	FIBER LAYER
Mean:	31.047	66.246
N. of points:	39	39
Std deviation:	11.168	33.527
Std error:	1.788	5.369
Minimum:	17.117	27.251
Maximum:	60.181	156.69
Median:	26.656	63.456
Lower 95% CI:	27.425	55.373
Upper 95% CI:	34.668	77.118

Table 3. Data summary from the comparison in N-Cadherin content between perivascular and periaxonal astrocytes.

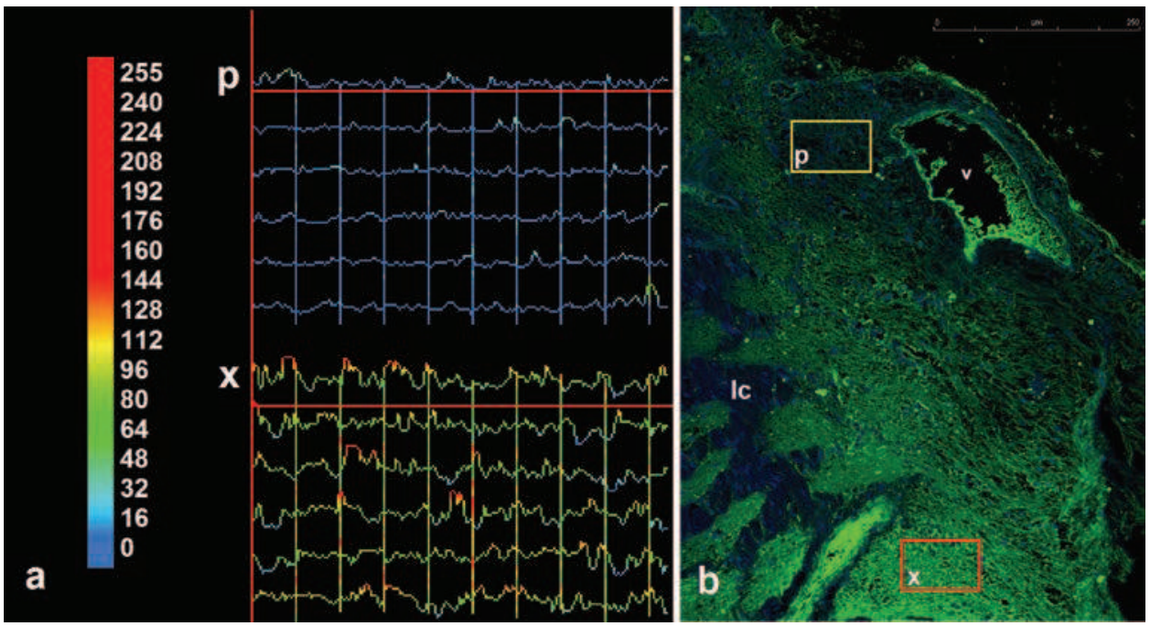

Fig. 6. a) False color scale and curves from data measured in b. Data taken from six lines in squares p and x is printed graphically as a curve where the color hue indicates the pixel intensity according to the conventional scale that is depicted on the far left. b) CLSM photograph of immunofluorescence staining against N-cadherin in the optic-nerve head. At the top, the image shows one of the central vessels (v) surrounded by Elschnig's astrocytes; and, on the left, part of the lamina cribrosa sclerae (lc). The squares show two typical locations where fluorescent intensity is measured along six lines. The square marked p is located in the perivascular region where Elschnig's astrocytes are found. The square marked x is located in the area of axon bundles. The measurements on the squares are represented graphically in a). (Vit: Vitreous body; V: Vessel; A: Astrocytes; FL: Fiber layer; lc: lamina cribrosa).

drawn in the perivascular area and fiber layer showed that the N-cadherin concentration was greater in the fiber area (Figure 7). The two-tailed p-value was < 0.0001 (considered extremely significant).

In summary, the axon-laden region of the prelaminar tissue was rich in N-cadherin compared to the perivascular region. This confirms the impression conveyed by the TEM micrographs, which show more numerous figures of zonulae adherens among the astrocytic projections surrounding axon fibers.

3.2.5 The presence of four molecules related to the lactate shuttle in the prelaminar region of the optic nerve head

Qualitative assessment of LDH 1 staining was positive. The presence of the molecule was best denoted in the fiber layer, indicating its presence in the astrocyte-axon couple. Figure 8a shows a case of LDH 1 and the corresponding negative control.

Qualitative assessment of LDH 5 staining was positive. Fluorescence is detected in the astrocyte-axon in the region of the tightly packed axon bundles. Figure 8b shows a case of LDH 1 and the corresponding negative control.

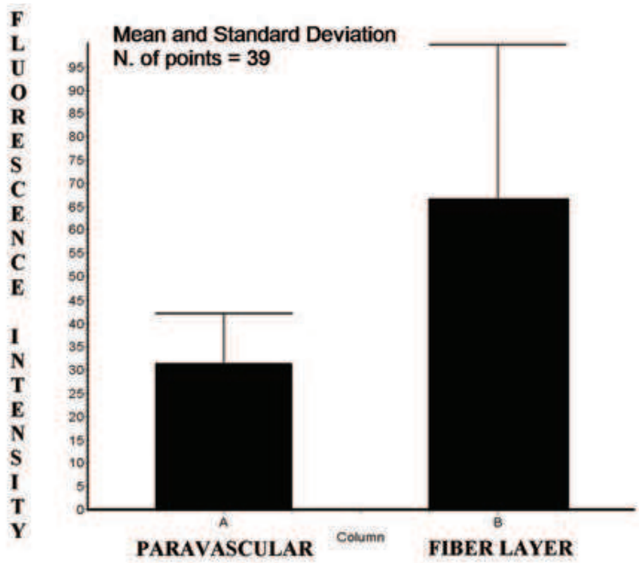

Fig. 7. Comparison of the fluorescent intensity of anti-N-cadherin antibodies in the perivascular area and in the nerve-fiber layer: the bars represent the mean of the fluorescence intensity in each area. The standard deviation is also included. The y-axis depicts the intensity scale in arbitrary units.

CLSM immunofluorescent labeling of MCT 1 was weakly positive in the astrocyte-axon of the prelaminar tissue. This presence of this molecule was best denoted in the fiber layer, while in other areas it was barely detectable (Figure 8c). The same labeling of MCT 2 was also weakly positive in the prelaminar tissue and its presence was clearest in the fiber layer, indicating its presence in the axon-astrocyte couple (Figure 8d). Due to the weak fluorescence of MCTs, we used the optic nerve from Wistar rats as a positive control and confirmed the correct labeling of the targets while excluding species disparity in the specificity of the primary antibodies (not shown).

3.2.6 TEM immunogold of MCT1 and MCT2

After the detection of MCT1 and 2 under light microscopy, it was necessary to localize the molecules in the plasma membranes to confirm their metabolic role in the lactate shuttle between astrocytes and neurons. Both molecules were localized mainly in the plasma membranes in both cell types. MCT1 was also localized in the inner mitochondrial membrane (not shown). TEM immunogold labeling of MCT1 showed the distribution of MCT1 molecules in the astrocyte membrane near the axon membrane (Figures 9a, b, c). TEM immunogold labeling of MCT2 revealed the distribution of MCT2 molecules in the axon membrane near the astrocyte membrane, as well as in the astrocyte membranes surrounding the axons (Figures 10a and b). Immunogold was also present in the numerous thin astrocytic projections that filled extra-axonal spaces and which were not in contact with the axon membrane. This occurred with both MCT1 and MCT2 (Figures 9c and 10b).

In summary, the enzyme isoforms, LHD 1 and LDH 5 were detected in the prelaminar tissue, and the staining was more intense in areas where axons joined to pierce the lamina cribrosa sclerae. Both of the monocarboxylate transporters studied here (MCT1 and 2) were located in the plasma membrane of the astrocyte-axon couple. Together, these four molecules formed part of a chain in the metabolic link between astrocytes and neurons.

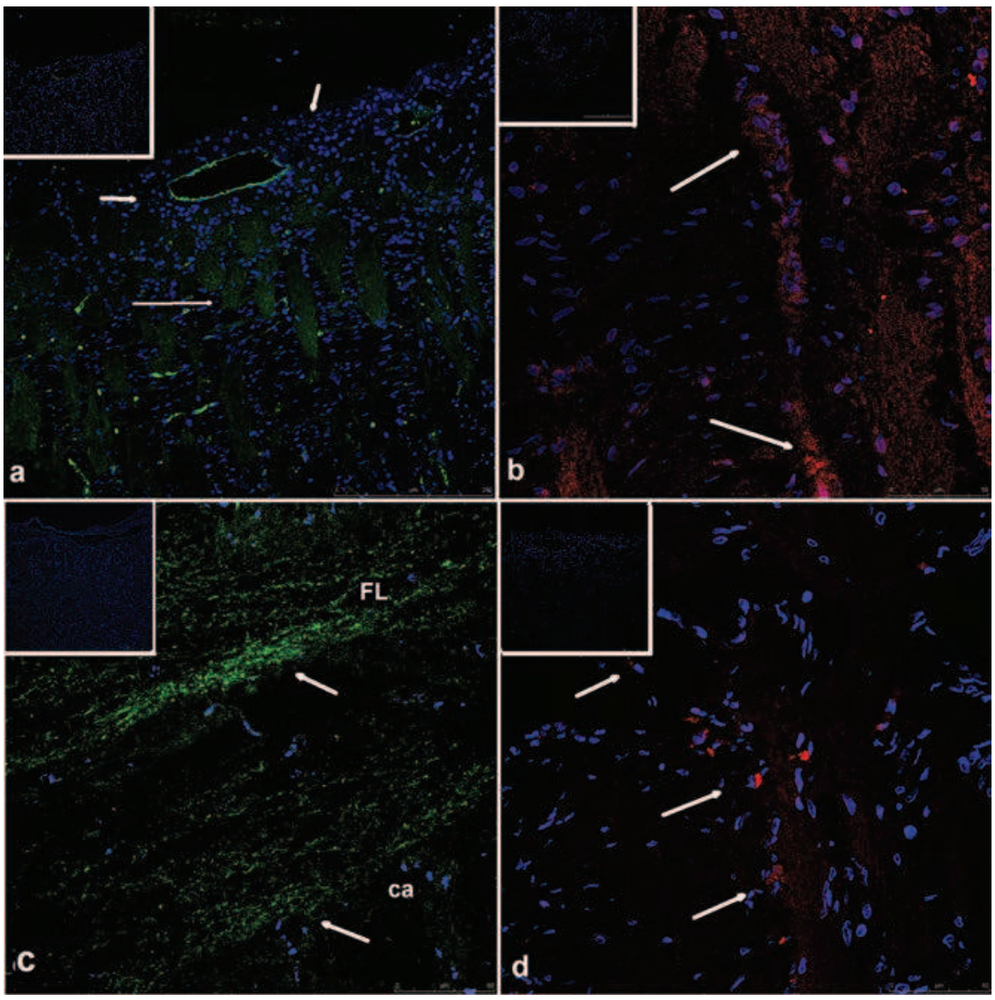

Fig. 8. a) CLSM micrograph of the optic-nerve-head-labeling LDH1 with fluorescein (green color, FITC). Immunostaining is positive in the nerve-fiber layer (long arrow) and less intense in the perivascular astrocytes (short arrows). (Insert) Negative control of LDH1 antibody. Secondary fluorescent anti-FC fraction antibody is used without previous incubation with the primary antibody. Both images have been taken with the same parameters of laser intensity and aperture. b) CLSM micrograph of the optic-nerve-head-labeling LDH 5 (red color, TR). Labeling is intense in the fiber bundles near and inside the cribrosa lamina (arrows). (Insert) Negative control of LDH5 antibody. (**Vit**: Vitreous body; **V**: Vessel; **ca**: Columnar astrocytes; **lc**: Lamina cribrosa). c) CLSM micrograph of the optic-nerve-head-labeling MCT1 with fluorescein (green color, FITC). Green immunostaining is positive in the astrocytes-axon couple (arrowed) and located in the nerve-fiber layer. (Insert) Negative control of MCT1 antibody. Secondary fluorescent anti-FC fraction antibody is used without previous incubation with primary antibody. Both images were taken with the same laser intensity and aperture to the change in magnification. d) CLSM micrograph of the optic-nerve-head-labeling MCT 2 (red color, TR). Red immunostaining positive in the astrocytes-axon couple. Staining was more detectable at the level of the lamina cribrosa. Insert: Negative control of MCT 2 antibody. (**FL**: Fiber layer; **ca**: Columnar astrocytes; **lc**: Lamina cribrosa).

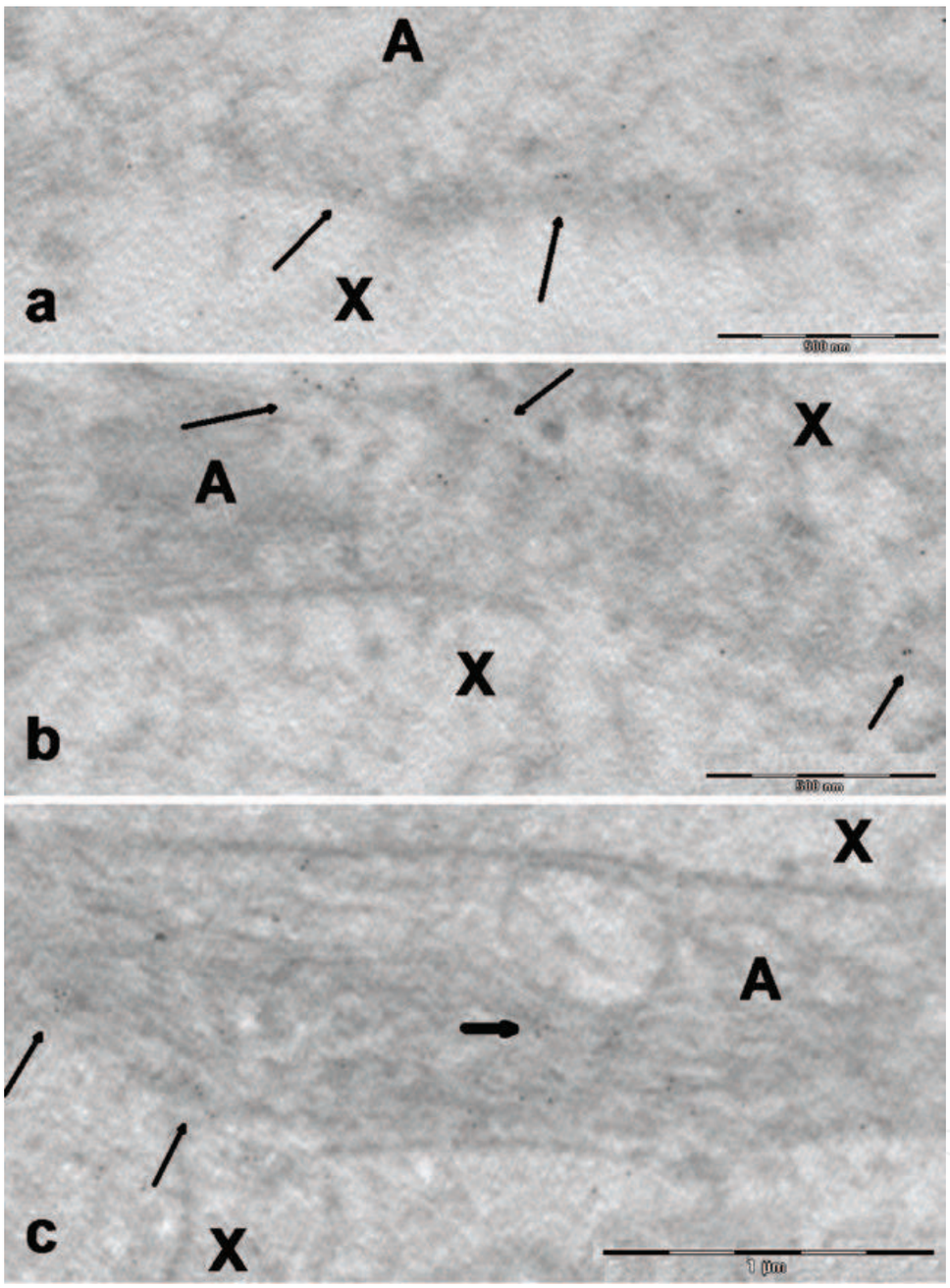

Fig. 9. TEM micrograph of the fiber layer of the optic-nerve head immunolabeled with anti-MCT1 antibody and immunogold. Membranes are not easily seen with this technique, as electron-dense contrast is avoided so that the gold micelles are not masked. **a**, **b**, and **c** are different samples in which specific markings of MCT1 are deduced from the delineation of the membranes by the marker (long arrows). The short arrow points to the multi-layered projections as seen in Figure 4b and c. X indicates axon; and A indicates astrocyte. A distinction between astrocytic projections and axons is established by the shape and presence of intermediate filaments. Ultra-thin sections, as well as osmium tetroxide-free and uranyl acetate, counterstain without lead citrate. Magnification is shown in the figure.

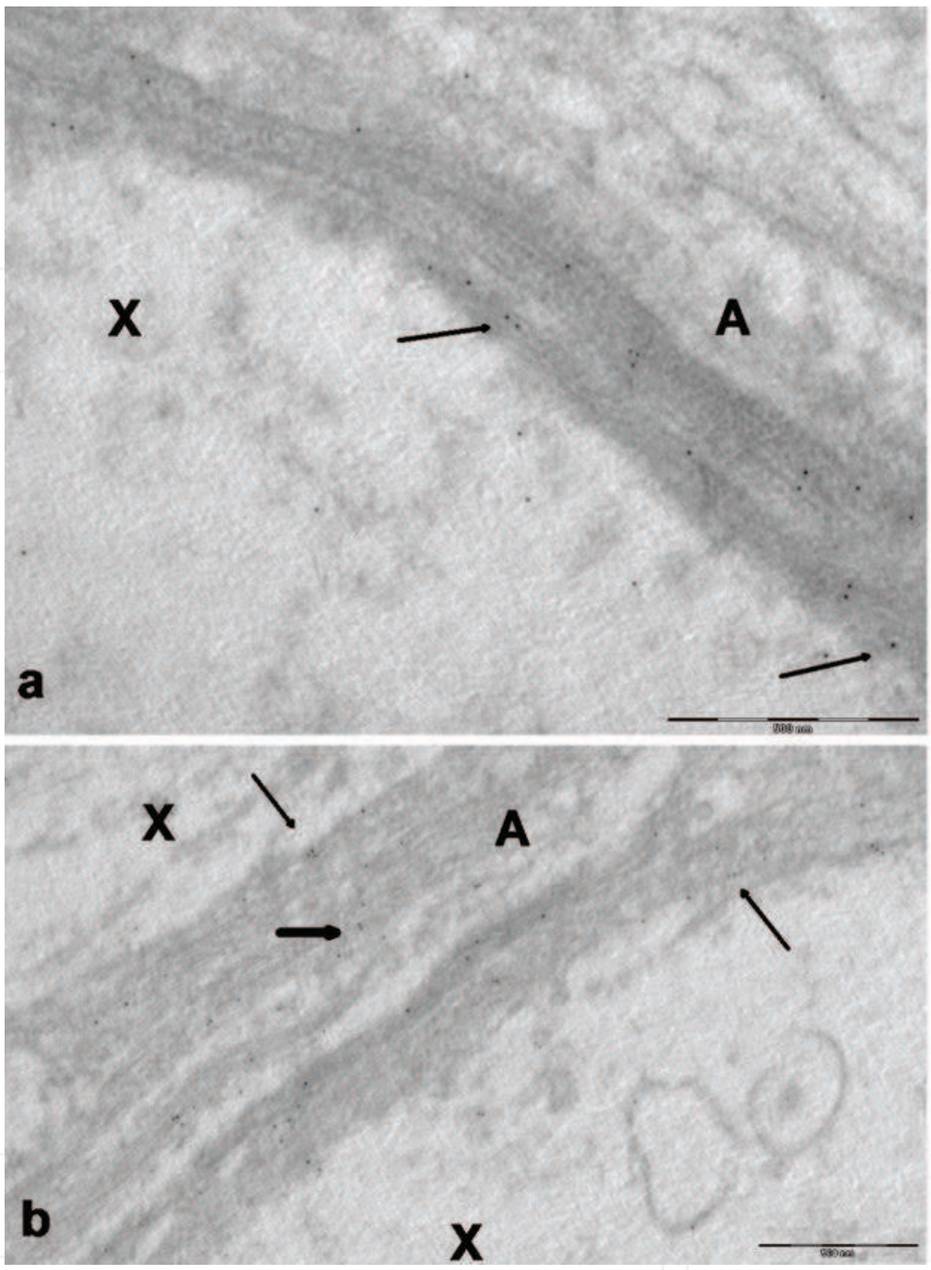

Fig. 10. TEM micrograph of the fiber layer of the optic-nerve head immunolabeled with anti-MCT2 antibody and immunogold. As in Figure 10, membranes are not easily seen in these sections because they have been processed without electron-dense contrast (so as not to mask the gold micelles). **a** and **b** are different samples in which specific markings of MCT2 are deduced by the delineation of the membranes by the marker (long arrows) in the astrocytic membrane. The short arrow points to the presence of MCT2 in the membrane of multi-layered projections that fill extra-axonal spaces. This suggests lactate re-uptake on the part of the astrocytes, the **X** axon, and the A astrocyte. Ultra-thin sections, as well as osmium tetroxide-free and uranyl acetate, counterstain without lead citrate. Magnification is shown in the figure.

3.3 Organotypic culture

3.3.1 Morphology

We cultured samples of the prelaminar optic nerve up to 12 days. The samples were studied and labeled for neurofilament and GFAP daily for the first 6 days of culture and twice daily afterwards.

The persistence of healthy astrocytes in organotypic culture of the prelaminar optic nerve is illustrated in Figure 11 a to c. Even on day 12 of the culture, astrocytes were found with regular features of nuclei and GFAP labeling (Fig 11 c). The mass reduction of the culture tissue detected over the culture process indicates that astrocytes are also regularly lost, as confirmed by the presence of pycnotic nuclei in some portions of the sections (Figure 11e

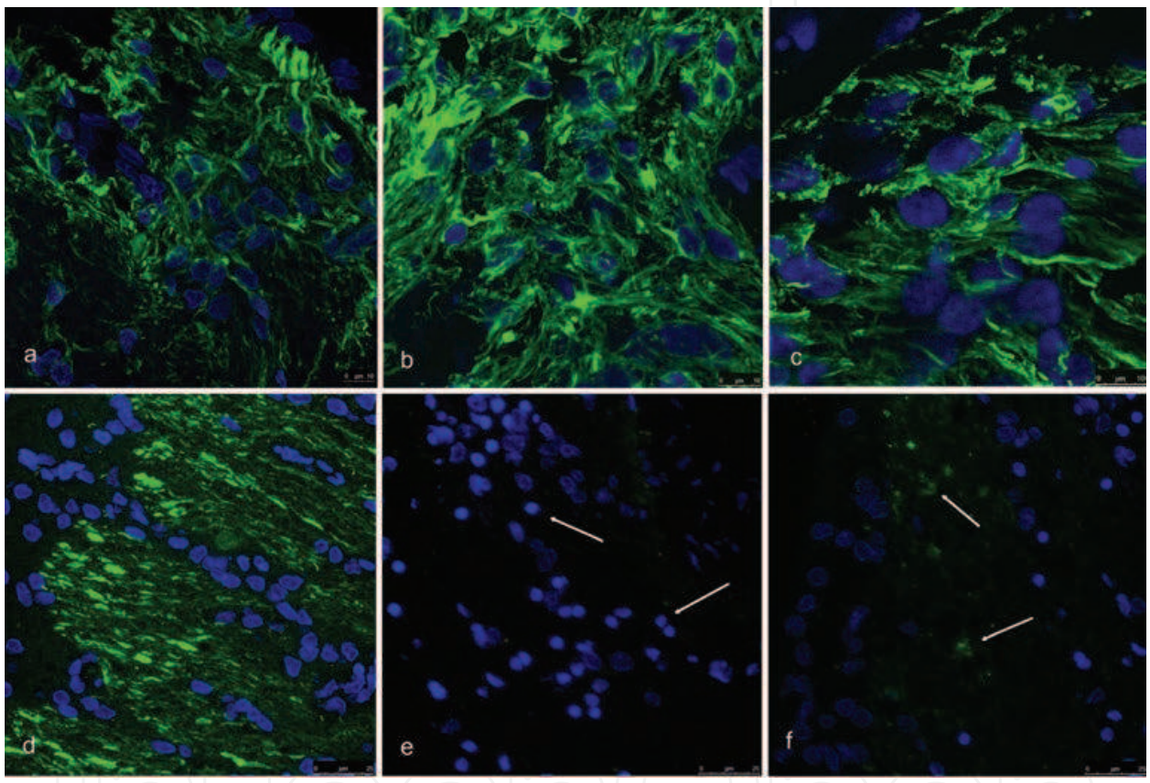

Fig. 11. CLSM micrographs of immunolabeled tissue. Upper row shows the fate of astrocytes in culture by the morphology of GFAP filaments and nuclear staining with DAPI. The lower row shows the fate of axons after one day of culture by the labeling of neurofilament. Nuclear staining with DAPI. a) GFAP Control, in cultured tissue. b) GFAP after 4 days of culture. Normal appearance of nuclei and GFAP filaments. c) GFAP after 12 days of culture. Normal aspect of remaining nuclei. GFAP is still abundant in the cytoplasm with signs of clumping is some areas. d) CLSM micrography Control preparation of prelaminar optic-nerve head in a non-cultured sample. Immunolabeling with anti-neurofilament. Secondary antibody labeled with FITC. Paraffin embedding. d) Same immunolabeling in a prelaminar optic disc cultured for 24 h. Axons have completely disintegrated as shown by the absence of staining in the major part of the sample. f) Same preparation. Only traces of neurofilament are visible in some regions (arrows). Figures b and c show some nuclei are undergoing pycnosis (arrow head). Magnification shown in the figures.

and f) and aggregated GAFP in the cytoplasm of cells with pycnotic (not shown) or normal-appearing nuclei (Fig 11 c).
Neurofilament staining in cultured and control tissues showed that neurofilament was practically absent from the samples after one day culture onwards (Figure 11 d to e).

3.3.2 Protein immunoblotting

Western-blot analysis of MCT1 and MCT 2 after 1, 2, and 5 days of culture, when axons had already disintegrated allowed a quantitative comparison between cultured and control samples of both MCT1 and MCT2. An instance of the bands obtained are represented in figure 12. Astrocytes express 42±6% of the total amount of MCT1. Astrocytes express 57±17% of the total amount of MCT2. See Figure 12 for a sample of the Western blot's bands for MCT1 and MCT 2 along with thePonceau' protein staining.
Although the standard deviation is not small in the case of MCT2 (17%), due to intrinsic limitations in the methodology of western blot we cannot deduce those results exactly show the real expresion of MCT in axons and astrocytes in the normal tissue. Then we will discuss those results assigning to astrocytes around 40% of the total MCT1 and to axons the remaining 60%. In like manner, we can round up MCT2 content attributing to astrocytes 60% of the total and to axons the remaining 40% (Table 4).

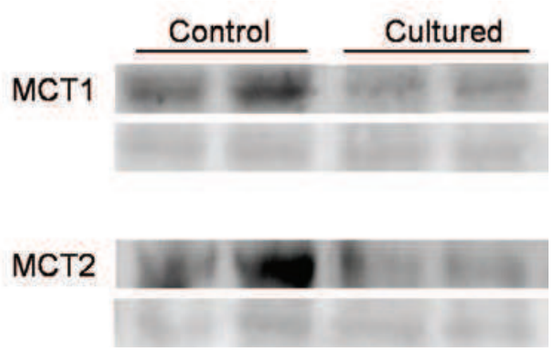

Fig. 12. Samples from Western blot analysis of cultured vs. uncultured prelaminar optic nerve of MCT1 and MCT2. Upper row shows immunolabeling and lower row shows protein staining with the Ponceau method to show the amount of protein content in the sample. Both figures show a reduction of the molecule in cultured tissue after axon removal. Both MCT1 and MCT2 are consequently expressed in axons and astrocytes alike. For quantitative results, see text.

	ASTROCYTE	AXON
MCT1 (percentage)	40%	60%
MCT2 (percentage)	60%	40%

Table 4. Distribution of MCT1 and MCT2 between astrocytes and axons after comparing fresh to cultured prelaminar optic nerve tissue (figures rounded up).

4. Discussion

We determined the presence of monocarboxylate transporters MCT1 and MCT2 in the prelaminar optic nerve head by Western blot, indicative of the activity of the lactate shuttle

in the area. Then, as the fluorescence and ultrastructural observation of the prelaminar optic nerve suggested that zonulae adherens and its main constituent, N-cadherin, were more prevalent in the bundles of nerve fibers and columnar astrocytes than in the perivascular astrocytes, we performed a statistical study of the distribution of N-cadherin in images of CLSM with fluorescent immunolabeling. This study showed N-cadherin to concentrate in the axon-astrocyte bundles. With the idea that adhesion structures such as zonulae adherens would contribute to the feasibility of the transport of lactate across the astrocyte-axons boundary, we colocalized in this area MCT isoforms 1 and 2 as well as LDH isoenzymes 1 and 5. Finally, culturing the prelaminar optic nerve for 1 to 5 days, we separated the population of astrocytes of the optic nerve head from the sectioned axons that disintegrated in the culture. Western-blot analysis of cultured vs. control prelaminar tissue rendered the proportion of MCT isoforms present in each cellular type, astrocytes and neurons (axons). Both MCT1 and MCT2 were present in astrocytes as well as the axons but in different proportions.

4.1 Western-blot bands

Information regarding the localization of the bands of porcine MCTs is somewhat conflicting. Welter and Claus (2008) point to the band of 41 kDa for MCT1 of porcine origin, while Santa Cruz Biotechnology situates MCT1 of human origin between 43 and 50 Kda, and Abcam Laboratories around 52 Kda. For MCT2 of human origin, Santa Cruz biotechnologies predicts a band in the 43 KDa mark, and Abcam in the band of 52 KDa. Our bands coincide with the data of Santa Cruz Technologies. The resulting bands were neatly marked, indicating a specific detection (Figures 1 and 12)

4.2 Morphology

The tissue structure of the fiber layers of the prelaminar optic nerve head is intricate. Numerous thin astrocytic projections intermingle with axons and other astrocyte projections, forming a mesh that defies the resolution power of fluorescent confocal laser microscopy. In this particular region, it is not possible to identify the type of cell in paraffin sections, even with the help of double-labeling. Target molecules are normally colocalized using an ancillary antibody directed against a molecule that helps identify the type of cell involved. A second problem arises when this technique is attempted in paraffin sections of our area of interest when the molecule to detect is present in small amounts in the tissue: if an intracellular target such as GFAP is used for astrocytes, or neurofilament for axons, the staining is so intense that it masks the weak fluorescence of the primary target molecule. As a result, instead of singling out individual cells with co-labeling, we considered the astrocyte-neuron couple as a functional unit from the standpoint of the lactate shuttle. For our purposes, it is sufficient to detect whether the molecules are present or absent in particular areas of the optic nerve head.

Accordingly, here we present our results with the single-staining technique. Our method was to use the control section without a primary antibody, to set the acquisition parameters of the microscope so that there was no background and the image was completely dark. Any fluorescence found when exploring the specimen with primary and secondary antibodies was considered positive if the anatomical distribution of the labeling was specific. The background was eliminated because the parameters were identical to control. This method enabled a qualitative evaluation of the results. The results were classified as negative or

positive (weak, moderate or intense). We interpreted weak positives to mean that the molecules being detecting were present in the tissue in very small amounts. We are dealing, in part, with transporting molecules floating in the cell membrane in very tiny amounts, surrounded by many different molecules sharing the membrane. Consequently, the resulting fluorescence were small.

Our results can be briefly described as showing that zonulae adherens in pig eyes are more abundant at sites having both the presence of astrocytes and axons than at astrocyte-only sites (perivascular astrocytes of Elschnig and Kuhnt). The areas of astrocyte-axon contact gave more intense results than did the perivascular areas when evidence of enzymes related to the lactate shunt was searched for. All four proteins —LDH 1, LDH 5, MCT 2, and MCT 1— were detected in the areas where astrocytes and neural fibers were densely packed, as occurs in the fiber layer of the optic nerve head near the lamina cribrosa. As shown in the TEM micrographs, astrocytic projections were firmly maintained in place around axons by closely situated zonulae adherens. This arrangement suggests that axon-wrapping astrocytic prolongations may play a role in facilitating the lactate shuttle, for which a narrow and stable (in relation to space) extracellular gap is a precondition. Disruption of this equilibrium may have pathological consequences. As suggested above, a misdirection of the aqueous humor outflow that subsequently interferes with N-cadherin attachments may alter the relationship between the lactate shuttle and the narrow intercellular spaces (Carreras et al., 2009).

Optic-nerve-head astrocytes are believed to be controllers of the development of the retinal vasculature in mammals. Around birth, astrocytes in the optic-nerve head spread across the inner surface of the retina (Watanabe, 1998) and act as a template for the developing retinal vasculature. This retinal development (Fruttiger, 2002) is controlled by a hierarchy of interactions among retinal neurons, astrocytes, and blood vessels. Retinal neurons stimulate a proliferation of astrocytes which in turn stimulate blood-vessel growth, and the developing vessels then provide feedback signals that trigger astrocyte differentiation, and vessel growth is stopped (West et al., 2005). The astrocytes in the center of the disc and accompanying the main central trunks (known as the meniscus of Kuhnt and Elschnig's astrocytes) surround the central branches and form the incomplete inner limiting membrane (ILM). These astrocytes can be considered as a functional unit. Axon-wrapping astrocytes form another functional group, providing support for the neurons.

In the TEM micrographs, we found that the figures for zonula seemed to be more numerous among those astrocyte projections that tightly surround axons in the fiber layers of the optic nerve head. To test this hypothesis, we performed many immunolabeling sections using eyes from different pigs and comparing the immunolabeling intensity among perivascular astrocytes with axon-related astrocytes. The possibility that the difference between the groups was due to sampling has a probability of less than one in 10,000 ($p < 0.0001$). Our results show that N-cadherin, and consequently zonulae adherens, were more numerous in the proximity of the axons. This may indicate the importance of membrane contact and narrow extracellular spaces in the axon-astrocyte relationship.

4.3 Lactate shuttle enzymes

The results of this study demonstrate that the isozymes LDH1 and LDH5 were present in the astrocyte-axon of the prelaminar tissue of the optic nerve head. From what is known about the kinetics of LDH, these results are compatible with the concept of the participation

of such a group of isozymes in lactate production in astrocytes and energy metabolism in axons.

The interconversion of lactate and pyruvate is catalyzed by the enzyme lactate dehydrogenase. The LDH-5 subunit (muscle type) tends to favor the formation of lactate from pyruvate. The LDH-I subunit (heart type) preferentially leads toward the production of pyruvate. Isozymes of LDH, LDH1, and LDH5 are easy to separate antigenically because LDH1 is formed by four H subunits and LDH5 by four M subunits. All isoenzymes are present in different proportions in all the processes, but the differences may be sufficient to be brought about by immunostaining. It has been found (using immunohistochemistry techniques on the occipital cortex of rats) that neurons contain mainly the LDH1 subunit, while astrocytes contain both isozymes. These observations support the notion of a regulated lactate flux between astrocytes and neurons (Bittar et al, 1996).

The concept of the cell-cell lactate shuttle implies that the production and exchange of lactate is a major means of providing energy to the cell. A related notion, the intracellular lactate shuttle, states that the mitochondria are sites of lactate oxidation by lactate dehydrogenase (LDH) (Passarella et al., 2008). Examples of cell-cell shuttles include lactate exchanges between astrocytes and neurons. Lactate exchange between production sites and removal is facilitated by monocarboxylate transport proteins, of which there are several isoforms. The presence of cell-cell and intracellular lactate shuttles shows that glycolytic and oxidative pathways are linked processes, in which lactate is the product of one pathway and the substrate for the other pathway (Brooks, 2009).

4.4 Organotypic culture and MCT distribution

Early destruction of axons in tissue culture of the prelaminar optic nerve is consequence of the sectioning of axons at the level of the peripapillary neuroretinal rim and at the level of the lamina cribrosa. In less than 24 h the remains of the axons were merely testimonial. Astrocytes may persist with normally distributed GFAP even after 12 days of culture, but nuclear pycnosis and GFAP clumping, probably a sign of blebbing, was present in the cultured tissue in variable amounts from day 1 with the method followed here. Because of the preservation of a large enough proportion of the astrocytes, a comparison of the relative amount of MCTs of a cultured prelaminar tissue relative to non-cultured fresh tissue is a means of ascertaining the distribution of the two molecular types between the two cell types involved, astrocytes and neurons. After one day of culture, one population of astrocytes was well preserved, while axon membranes were completely absent. Only scant remains of neurofilaments dispersed in some regions of the sample ensured that one-day-old cultures were adequate to quantify the expression of MCTs in the membrane of astrocytes (Figure 11).

Fourteen MCT isoforms and their specific tissue distribution have previously been identified in mammals. Four of these isoforms, MCT1-4, have also been shown experimentally to act as transmembrane transporters of lactate, pyruvate, and ketone bodies (Halestrap & Meredith, 2004). Distribution of MCT variants among cell types is not even. Broer et al. (1997) showed that cultures of astroglial cells contained mRNA encoding MCT1, but little mRNA encoding MCT2. Hanu et al. (2000) reported that neonate rat astrocytes in primary culture express significant levels of both MCT1 and MCT2, and confirmed previous results indicating that the expression of the two transporters is restricted to specific populations of astrocytes in the mature brain. The same cell may contain MCT1 and MCT2, as occurs with Müller cells. Gerhart et al. (1999), working on rat retinas, found that MCT-1 was expressed by the apical

processes of the retinal pigment epithelium as well as in endothelial cells, Müller-cell microvilli and in inner rod segments. MCT-2 was found to be expressed by Müller's cells and by glial cell processes surrounding retinal microvessels.

Debernardi et al. (2003) reported that in mouse-brain cortical-cell cultures that astrocytes strongly expressed MCT1 but had very little if any MCT2, at both the mRNA and the protein levels. By contrast, neurons had high amounts of MCT2 and low to moderate levels of MCT1. Thus, studies of cells *in vitro* and *in vivo* have yielded somewhat different results and, on the other hand, astrocytes and neurons can express different isomorphs of MCT in specific areas of the CNS. Consequently, each region of the CNS demands its specific study of the distribution of MCT. That distribution would speak of the role of both the neuron and the astrocyte in the regulation of lactate (and other monocarboxylates) in the intercellular cleft. The extracellular lactate pool is increased by MCT 1 release and decreased by MCT2 intake, as the extracellular lactate concentration has been found to be approx. 1 mM in both rats and humans (Abi-Saab et al., 2002; Pellerin, 2005b).

Western-blot analysis of MCT1 and MCT 2 after 1, 2, and 5 days of culture, when axons had already disintegrated showed that both MCT1 and MCT2 were still present in the tissue. It indicated that MCT1 and MCT2 were present in the membrane of the astrocytes. Both MCT isoforms were present in equivalent proportions in astrocytes and axons alike. As indicated in Table 4, a 40-60% for MCT1 and a 60-40% for MCT2 are present in astrocytes and axons respectively.

In our results, astrocytes anchored MCT1 and MCT2 in their plasma membrane, and accordingly had the ability to move lactate into the extracellular spaces and also the resources to re-uptake it. Astrocytes were thus able to control the extracellular concentration of lactate near the axon. This is corroborated in Figures 9 and 10, in which the membranes of the axon and the astrocytic prolongations in direct contact with the axons are labeled in gold. Discrepancies between the strong presence of MCT2 in optic-nerve astrocytes and not in cortical astrocytes, as reported by Debernardi (2003), may be partially related to the coupling of synaptic activity to glucose utilization in the astrocyte. This role is marked by the presence of receptors for a variety of neurotransmitters in the astrocytic processes near synapses that can influence the intake of glucose by the vascular feet of the astrocytes (Pellerin, 2005b). In the white matter, as in the prelaminar optic nerve, where synapses are absent, the regulatory ability to control the pool of monocarboxylates in the intercellular cleft appears to be permanently shared by both sides, astrocytes and neurons (axons).

Whether it is the astrocyte or the neuron that is responsible for maintaining a stable lactate pool can be deduced from the presence the two transporter molecules in the membrane of each cell type . Our results indicate that, in the optic nerve head astrocytes, neurons express similar amounts of MCT1 and MCT2 in their membranes. Although it could seem improbable that the neuron returns the lactate that it uses as fuel back to the intercellular cleft under normal conditions, the possibility of this return exists, and a reverse neuron-to-astrocyte lactate shuttle has recently been proposed (Mangia et al., 2009). It bears mentioning here that, in addition to lactic acid transport, MCTs also mediate the transport of many other metabolically important monocarboxylates such as pyruvate, the branched-chain oxo acids derived from leucine, valine, and isoleucine as well as the ketone bodies (acetoacetate, hydroxybutyrate and acetate (Halestrap & Meredith, 2004)). Having the ability to expel unwanted metabolites via MCT1 is a plausible role for this molecule in the axonal membrane.

The fact that MCT 1 is present in the astrocyte and MCT2 appears in the axon membrane agrees with the results of Pellerin et al. (2005a) and other authors on cortical neurons (see Pellerin 2005b and 2007b for a review). However, the abundance (up to 60%) of MCT2 in astrocytes and MCT1 in neurons may be a feature of the optic nerve and perhaps white matter. It has been shown that, in the gray matter, levels of expression of MCT2 in the membrane can change in response to variable situations in order to adjust for energy requirements (Pellerin et al., 2007a). Metabolic requirements of cortical-cell activity are presumably more complex that mere axonal conduction, and the expression of similar amounts of MCT isoforms in the membranes of both astrocytes and neurons can be a regular feature, but this point needs to be assessed. In the optic nerve, Tekkok et al. (2005) corroborated previous works by their group that L-lactate is released from astrocytes and taken up by axons in an experimental setting with mice. In addition, immunocytochemical staining localized MCT2 predominantly in axons, and MCT1 predominantly in astrocytes. The limitations of immunolabeling alone, and even supplemented with TEM, discussed previously in this paper, prompted us to complement the morphological approach with tissue culture. Our results, although slightly divergent, do not contradict previous results but show that MCT2 is also present in astrocytes and MCT1 also present in neurons in considerable proportion. Previously, MCT2 had been localized on glial foot processes surrounding retinal vessels (Gerhart et al., 1999).

The conclusion that there is a coincidental distribution of metabolic coupling molecules and N-cadherin suggests a close relationship between the functions of both sets of molecules intervening in the metabolism of lactate. The presence of four essential components of the l-lactate metabolic chain suggests that the survival of the axon depends on the close membrane contact brought about by N-cadherin-mediated zonulae adherens. Closely apposed membranes are an important requisite for the transfer of lactate from astrocytes to neurons, and on this feature depends partially the concentration of lactate in intercellular spaces. These features are represented on the left side of Figure 13.

4.5 N-cadherin and apoptosis

Astrocytes support neurons by means of the uptake and release of neurotrophic factors and cytokines, such as NGF, TNFa, and bFGF, which are fundamental for the viability of neurons. In addition, astrocytes prevent neurotoxic levels of neuron-released glutamate and K^+ from accumulating in extracellular spaces (Tsacopoulos & Magistretti, 1996). Cell-adhesion complexes act as sensors and at the same time contribute to the adhesive process and to the transmission of signals that result in a variety of cellular responses. Indeed, adhesion receptors can modulate or activate intracellular signal-transduction pathways in several ways, such as by interacting with proteins that link adhesive structures to cellular cytoskeletal networks, or by directly activating enzymes on the inner surface of the plasma membrane (Brunton & McPherson, 2004).

N-cadherin is a calcium-dependent molecule because calcium ions occupy positions in the extracellular domain of the molecule that enable the homo-engagement of similar molecules in the opposite membrane. Attachment does not take place when there are low levels of calcium in extracellular spaces. The separation of zonulae adherens may have two important consequences: 1) The separation of the membranes may negatively affect the transport of lactate (and other molecules) that are fundamental for the neuronal metabolism.

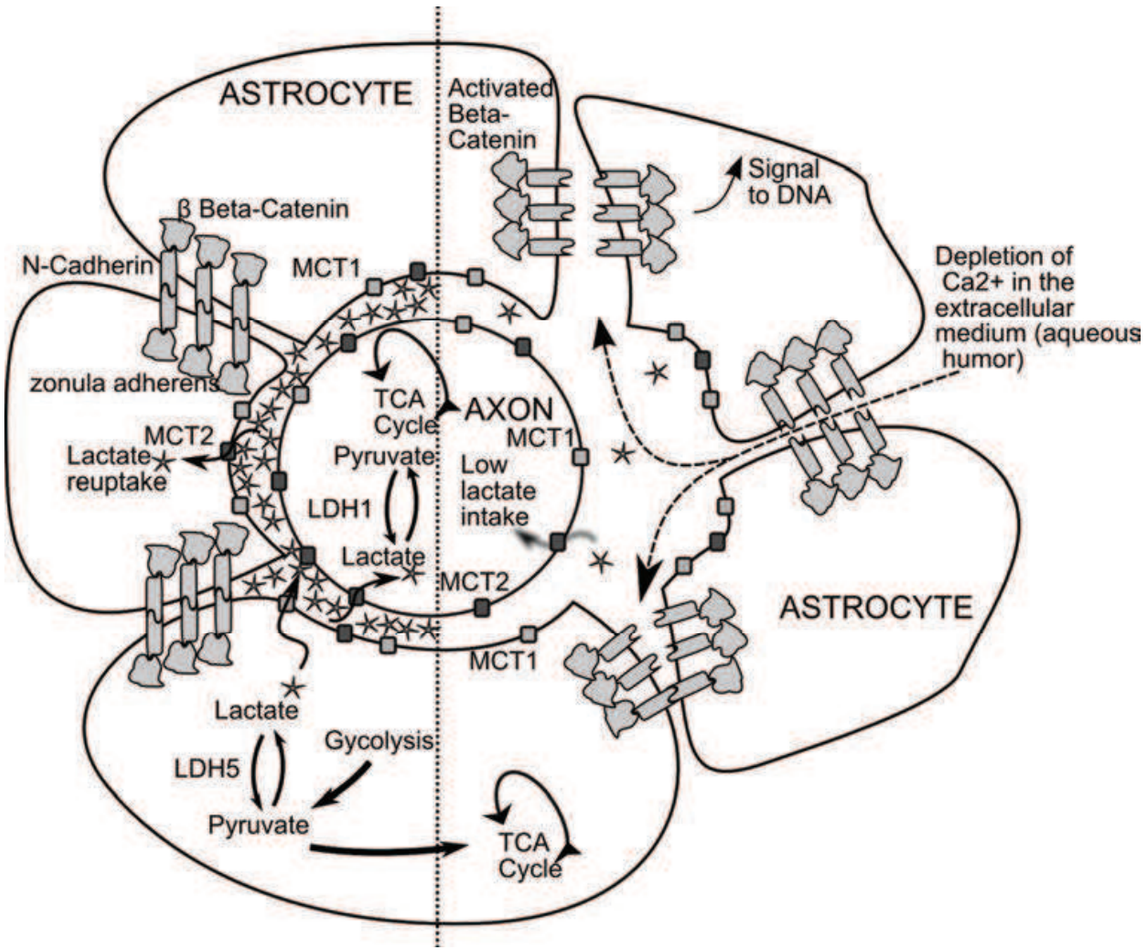

Fig. 13. Diagram of the relationships between the lactate shuttle and the membrane position through zonulae adherens in the axon and astrocytic projections. The left side shows physiological relationships: membranes are closely apposed by zonulae adherens. The main attachment complex is formed by N-cadherin, which is responsible for homotypic adhesion between the external surfaces of facing membranes. Beta catenin is known to be present on the inner side of the membrane. Catenins link the adherens junctions with the actin cytoskeleton. However, the catenins also transfer signals into and out of the cells, thereby mediating a variety of cell behavior such as proliferation, migration, differentiation, and death. Both carboxylate transporters MCT1 and MCT2 are present in axons and astrocytes. The right half of the diagram represents the hypothetical effects of aqueous humor flowing through the fiber layer of the optic nerve. The low calcium content of aqueous humor (roughly half the plasma concentration) could hypothetically wash away the calcium from sites in the N-cadherin molecule and lead to a separation of the zonulae adherens. Here the icon of beta catenin rotates to represent the activation of the signaling activity after the detachment of N-cadherin. Beta catenin signaling may trigger molecular cascades conducive to cell migration and/or apoptosis of the astrocyte. Increased extracellular spaces interfere with the dynamics of the lactate shuttle. Low lactate intake and the absence of astrocytes eventually determine the fate of the axon. This mechanism may play a role in the pathogeny of glaucomas, but a confirmation that the concentration of calcium ion in the aqueous is low enough to cause astrocytic detachment and/or apoptosis needs to be experimentally tested.

Extracellular spaces must have a critical volume for the adequate exchange of lactate. Abnormally increased extracellular spaces may interfere with the correct concentration of lactate and other molecules that must be incorporated into the cell (neuron) at a sustained rate, the dynamic of which is concentration dependent. The interruption of this chain may trigger axonal compartmentalized self-destruction (Whitmore, 2005). 2) Loosening the intermembrane attachment might compromise the information capabilities of this type of junction (Gumbiner, 1996). It has been shown that the blocking of N-cadherin-mediated intercellular interaction increases the number of cells undergoing apoptosis (Li et al., 2001). Messages are carried to the nucleus of the astrocyte and these may precipitate the mechanisms of cell migration (Nakagawa & Takeichi, 1998) and/or apoptosis (Makrigiannakis et al. 2000; Peluso et al., 1996). This doubly harmful effect could explain the disappearance of axons as well as astrocytes by two separate mechanisms related to the depletion of calcium ions. These features are represented on the right side of Figure 13.

5. Conclusion. Optic nerve architecture and glaucoma

Unlike epithelial-type cells, mesenchymal cells, of which astrocytes are an example, do not form impermeable barriers. Cell unions are invariably lax and therefore fluid can circulate between them (Adams & Nelson, 1998). Astrocytes and axons of the retinal ganglion cells are the main components of the optic nerve head. The structure of the anterior interface of the optic nerve has recently been revised. Simple membrane apposition is the main cell-attachment mechanism in the vitreous interface, and zonulae adherens is the only attachment junction among astrocytes (Carreras et al., 2009). The cell architecture enables the unimpeded passage of fluids from the vitreous cavity because of the complete absence of tight junctions (Carreras et al., 2010a 2010b).

The surface of the optic nerve in contact with the vitreous is uneven with respect to the penetration of fluids. As mentioned above, no sealed membrane exists and the entire surface is permeable. However, the presence of preferential flow routes in the perivascular region suggests that small quantities of fluid follow the perivascular route. (Carreras et al., 2010a). If the flow of fluid supersedes the ability of the preferential (or lymphatic-like) routes to evacuate, then aqueous humor from the anterior segment would reach the axon layers and interfere with the intermembrane contacts and its signaling activities. The pattern of visual field defects in glaucoma has been reproduced in a computer model that simulates progressive damage affecting the optic-nerve head from the vitreous (anteroposteriorly), as would be caused by the diverted flow of aqueous humor (Carreras et al., 2011).

In summary, the aqueous flow through the prelaminar tissue may interfere with the astrocyte-axon relationship in more than one way. An increase in the intermembrane gap and a simple washout of the extracellular lactate would directly interfere with the kinetics of monocarboxylate uptake. Low calcium-ion concentration, a hallmark of aqueous composition, may interfere with the cadherin attachments and increase separation. Moreover, messenger activity by zonulae adherens may trigger signals conducive to apoptosis. This mechanism may play a role in the pathogeny of glaucomas, but a confirmation that the concentration of calcium ion in the aqueous is low enough to cause astrocytic detachment and/or apoptosis needs to be experimentally tested.

6. Acknowledgments

Authors wish to thank Carmen Ruiz and Juan de Dios Bueno for their technical assistance.

7. References

Abi-Saab WM, Maggs DG & Jones T. Striking differences in glucose and lactate levels between brain extracellular fluid and plasma in conscious human subjects: effects of hyperglycemia and hypoglycemia. Journal of Cerebral Blood Flow & Metabolism. 2002; 22: 271–279.

Adams CL & Nelson WJ. Cytomechanics of cadherin-mediated cell-cell adhesion. Current Opinion in Cell Biology. 1998; 10:572-7.

Alma A & Nilsson SFE. Uveoscleral outflow – A review. Experimental Eye Research. 2009; 88:760-768

Aubert A, Costalat R, Magistretti PJ & Pellerin L. Brain lactate kinetics: Modeling evidence for neuronal lactate uptake upon activation. PNAS. 2005; 102:16448–16453

Bittar PG, Charnay Y, Pellegrin L, Bouras C & Magistretti PJ. Selective distribution of lactate dehydrogenase isoenzymes in neurons in astrocytes of human brain. . Journal of Cerebral Blood Flow & Metabolism. 1996; 16:1079-1089

Broer S, Rohman B, Pellegri G, Pellerin L, Martin JL, Verleysdonk S, Hamprecht B, & Magistretti PJ. Comparison of lactate transport in astroglial cells and monocarboxylate transporter 1 (MCT1) expressing Xenopus laevis oocytes. The Journal of Biological Chemistry 272: 30096–30102, 1997.

Brooks GA. Lactate shuttles in nature. Biochemical Society Transactions. 2002; 30:258–264.

Brooks GA. Cell–cell and intracellular lactate shuttles. The Journal of Physiology. 2009; 587: 5591–5600.

Brown AM, Tekkök S B & Ransom BR. Energy transfer from astrocytes to axons: the role of CNS glycogen. Neurochemistry International. 2004; 45:529-536.

Brunton VG, MacPherson IRJ & Frame MC. Cell adhesion receptors, tyrosine kinases and actin modulators: a complex three-way circuitry. Biochimica et Biophysica Acta. 2004; 1692: 121-144

Carrasco MC, Navascués J, Cuadros MA, Calvente R, Martín-Oliva D, Santos AM, Sierra A, Ferrer-Martín RM & Marín-Teva JL. Migration and ramification of microglia in quail embryo retina organotypic cultures. Developmental Neurobiology. 2010 OI:10.1002/dneu.20860

Carreras FJ, Porcel D, Alaminos M & Garzon I. Cell-cell adhesion in the prelaminar region of the optic nerve head: a possible target for ionic stress. Ophthalmic Research 2009; 42:106–111.

Carreras FJ, Porcel D & Muñoz-Avila JI. Mapping the Surface Astrocytes of the Optic Disc: A Fluid-conducting Role of the Astrocytic Covering of the Central Vessels. Clinical & Experimental Ophthalmology. 2010; 38:300-308.

Carreras FJ, Porcel D, Guerra- Tschuschke I & Carreras I. Fenestrations and preferential flow routes in the prelaminar optic nerve through wet-SEM and perfusion of tracers. Clinical & Experimental Ophthalmology. 2010 ; 38:705-717.

Carreras FJ, Rica R, Delgado A. Modeling the patterns of visual field loss in glaucoma. Optometry and Vision Science. 2011; 88:63-79.

Fruttiger M. Development of the mouse retinal vasculature: angiogenesis versus vasculogenesis. Invest Ophthalmol Vis Sci. 2002; 43:522-527.

Debernardi R, Pierre K, Lengacher S, Magistretti PJ, Pellerin L. Cell-specific expression pattern of monocarboxylate transporters in astrocytes and neurons observed in different mouse brain cortical cell cultures. J Neurosci Res 200; 373:141–155

Gerhart DZ, Leino RL, Drewes LR. Distribution of monocarboxylate transporters MCT1 and MCT2 in rat retina. Neuroscience. 1999; 92:367-375.

Gumbiner BM. Cell adhesion: the molecular basis of tissue architecture and morphogenesis. Cell. 1996; 84:345-57.

Halestrap, A. P.; Meredith, D. The SLC16 gene family —from monocarboxylate transporters (MCTs) to aromatic amino acid transporters and beyond. Pflugers Arch. 2004, 447, 619−628.

Halestrap AP, Meredith D. The SLC16 gene family-from monocarboxylate transporters (MCTs) to aromatic amino acid transporters and beyond. Pflugers Arch. 2004; 447:619-628.

Hanu R, McKenna M, O'Neill A, Resneck WG, Bloch RJ. Monocarboxylic acid transporters, MCT1 and MCT2, in cortical astrocytes in vitro and in vivo. Am J Physiol Cell Physiol May 2000; 278:C921-C930

Li G, Satyamoorthy K, Herlyn M. N-Cadherin-mediated Intercellular Interactions Promote Survival and Migration of Melanoma Cells. Cancer Res. 2001; 61:3819-3825Morgello S, Uson RR, Schwartz EJ, Haber RS. The human blood–brain barrier glucose transporter (GLUT1) is a glucose transporter of gray matter astrocytes. Glia. 1995; 14: 3–54.

Makrigiannakis A, Coukis G, Blaschuk O, Coutifaris C: Follicular atresia and luteolysis. Evidence for a role for N-Cadherin. Ann NY Acad Sci. 2000; 900: 46-55.

Mangia S, Simpson IA, Vannucci SJ, Carruthers A. The in vivo neuron-to-astrocyte lactate shuttle in human brain: evidence from modeling of measured lactate levels during visual stimulation. J Neurochem. 2009; 109 Suppl 1:55-62.

Nakagawa S, Takeichi M. Neural crest emigration from the neural tube depends on regulated cadherin expression. Development. 1998; 125:2963-71.

O'Brien J, Kla KM , Hopkins IB, Malecki EA, McKenna MC. Kinetic Parameters and Lactate Dehydrogenase Isozyme Activities Support Possible Lactate Utilization by Neurons. Neurochem Res. 2007; 32:597-607

Passarella S, Bari L de, Valenti D, Pizzuto R, Paventi G, Atlante A. Mitochondria and L-lactate metabolism. FEBS Letters. 2008; 582:3569-3576

Pellerin L, Magistretti PJ.Glutamate uptake into astrocytes stimulates aerobic glycolysis: a mechanism coupling neuronal activity to glucose utilization. Proc Natl Acad Sci USA.1994; 91:10625–10629.

Pellerin L, Begersen L, Halestrap AP, Pierre K. Cellular and subcellular distribution of monocarboxylate transporters in cultured brain cells and in the adult brain. J. Neurosci. Res,2005a;. 79: 55–64.

Pellerin L. How astrocytes feed hungry neurons. Molecular Neurobiology2005b; 32: 59–72.

Pellerin L, Bouzier-Sore AK, Aubert A, et al. Activity-dependent regulation of energy metabolism by astrocytes: an update. Glia. 2007a; 55:251–1262.

Pellerin L, Bouzier-Sore AK, Aubert A, Serres S, Merle M, Costalat R and Magistretti PJ. Activity-dependent regulation of energy metabolism by astrocytes: an update. Glia 2007b; 55:1251-1262.

Peluso JJ, Pappalardo A and Trolice MP. N-cadherin-mediated cell contact inhibits granulosa cell apoptosis in a progesterone-independent manner. Endocrinology. 1996; 137:1196-1203.

Poitry-Yamate CL , Poitry S. Tsacopoulos M. Lactate Released by Miiller Glial Cells Is Metabolized by Photoreceptors from Mammalian Retina. J Neurosci. 1995; 15:5179-5191.

Redies C, Takeichi1 M. N- and R-cadherin expression in the optic nerve of the chicken embryo. Glia. 1993; 8: 161–171.

Schurr A. Lactate: the ultimate cerebral oxidative energy substrate? J Cereb Blood Flow Metab. 2006; 26:142–152.

Smith D, Pernet A, Hallett WA, Bingham E, Marsden PK, Amiel SA. Lactate: a preferred fuel for human brain metabolism in vivo. J Cerb Blood Flow Metab. 2003; 23:658-64.

Stoppini, L., Buchs, P. A., Muller, D., "A simple method for organotypic cultures of nervous tissue" J Neurosci Meth. 1991; 37:173–82.

Tekkok SB, Brown AM, Westenbroek R, Pellerin L, Ransom BR (Sep 2005) Transfer of glycogen-derived lactate from astrocytes to axons via specific monocarboxylate transporters supports mouse optic nerve activity., Journal of Neuroscience Research, 81 (5), 644-52.

Tsacopoulos M and Magistretti PJ. Metabolic coupling between glia and neurons. J. Neurosci. 1996; 16:877-885

Wanga DD, Bordey A. The astrocyte odyssey. Progress in Neurobiology. 2008; 86:342–367.

Watanabe T, Raff MC. Retinal astrocytes are immigrants from the optic nerve. Nature. 1988; 332:834-837.

Welter H, Claus R. Expression of the monocarboxylate transporter 1 (MCT1) in cells of the porcine intestine. Cell Biol Internat. 2008; 32:638-645.

Whitmore AV, Libby RT, John SWM. Glaucoma: Thinking in new ways--a rôle for autonomous axonal self-destruction and other compartmentalised processes? Prog Ret Eye Res. 2005; 24:639-662.

West H, Richardson WD, Fruttiger M. Stabilization of the retinal vascular network by reciprocal feedback between blood vessels and astrocytes. Development 2005; 132:1855-1862.

Yu S, Ding WG,. The 45 kDa form of glucose transporter 1 (GLUT1) is localized in oligodendrocyte and astrocyte but not in microglia in the rat brain. Brain Res. 1998; 797:65–72.

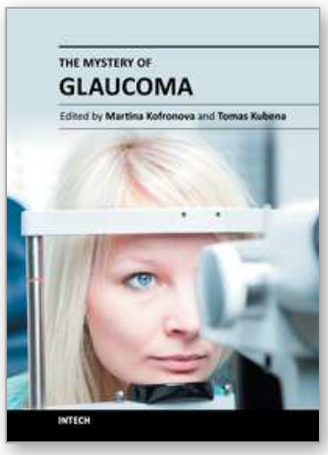

The Mystery of Glaucoma
Edited by Dr. Tomas Kubena

ISBN 978-953-307-567-9
Hard cover, 352 pages
Publisher InTech
Published online 06, September, 2011
Published in print edition September, 2011

Since long ago scientists have been trying hard to show up the core of glaucoma. To its understanding we needed to penetrate gradually to its molecular level. The newest pieces of knowledge about the molecular biology of glaucoma are presented in the first section. The second section deals with the clinical problems of glaucoma. Ophthalmologists and other medical staff may find here more important understandings for doing their work. What would our investigation be for, if not owing to the people's benefit? The third section is full of new perspectives on glaucoma. After all, everybody believes and relies – more or less – on bits of hopes of a better future. Just let us engage in the mystery of glaucoma, to learn how to cure it even to prevent suffering from it. Each information in this book is an item of great importance as a precious stone behind which genuine, through and honest piece of work should be observed.

INTECH
open science | open minds

InTech Europe
University Campus STeP Ri
Slavka Krautzeka 83/A
51000 Rijeka, Croatia
Phone: +385 (51) 770 447
Fax: +385 (51) 686 166
www.intechopen.com

InTech China
Unit 405, Office Block, Hotel Equatorial Shanghai
No.65, Yan An Road (West), Shanghai, 200040, China
中国上海市延安西路65号上海国际贵都大饭店办公楼405单元
Phone: +86-21-62489820
Fax: +86-21-62489821

IntechOpen